

A Computational Study on the Insertion of N(^{2}D) into a C—H or C—C Bond: The Reactions of N(^{2}D) with Benzene and Toluene and Their Implications on the Chemistry of Titan

Marzio Rosi[1(✉)], Leonardo Pacifici[2], Dimitrios Skouteris[3], Adriana Caracciolo[2], Piergiorgio Casavecchia[2], Stefano Falcinelli[1], and Nadia Balucani[2]

[1] Dipartimento di Ingegneria Civile e Ambientale, Università degli Studi di Perugia, 06125 Perugia, Italy
{marzio.rosi,stefano.falcinelli}@unipg.it
[2] Dipartimento di Chimica, Biologia e Biotecnologie, Università degli Studi di Perugia, 06123 Perugia, Italy
leo.pacificil@gmail.com, adriana.caracciolo@yahoo.it, {piergiorgio.casavecchia,nadia.balucani}@unipg.it
[3] Master-Up, Via Sicilia 41, 06128 Perugia, Italy
d.skouteris@master-up.it

Abstract. The reactions between nitrogen atoms in their first electronically excited state ^{2}D with benzene and toluene have been characterized by electronic structure calculations of the stationary points along the minimum energy path. We focused our attention, in particular, to the channels leading to the imidogen radical for the first reaction implying the insertion of nitrogen into a C—H bond and to the NCH_3 radical for the second reaction implying the insertion of nitrogen into a C—C bond. The minima along these reaction paths have been characterized using different ab initio methods in order to find a reasonable compromise between chemical accuracy and computational costs. Our results suggest that, while for geometry optimizations even relatively low level calculations are adequate, for energies higher level of calculations are necessary in order to obtain accurate quantitative results, in particular when strong correlation effects are present.

Keywords: Ab initio calculations · Titan atmosphere · Chemistry of planetary atmospheres · Prebiotic chemistry · Astrochemistry · Astrobiology

1 Introduction

Titan, the largest moon of Saturn, is the only solar system object with a thick dinitrogen atmosphere, besides the Earth [1, 2]. The other components of its atmosphere are mainly simple hydrocarbons like CH_4, C_2H_6, C_2H_4 and C_2H_2, simple nitriles like HCN and HCCCN, H_2 and Ar. This atmosphere is reminiscent of the primeval atmosphere of Earth [3, 4]. The reactivity of these species is very relevant as suggested by the

© Springer Nature Switzerland AG 2020
O. Gervasi et al. (Eds.): ICCSA 2020, LNCS 12251, pp. 744–755, 2020.
https://doi.org/10.1007/978-3-030-58808-3_54

information provided by the NASA/ESA/ASI Cassini-Huygens mission [5] and the observations performed with the ALMA interferometer [6]. Among the species identified by Cassini Ion Neutral Spectrometer (INMS), benzene shows a relatively important mole fraction, being 1.3×10^{-6} at 950 km [7]. Solid benzene has been identified also on the surface of Titan [8]. Toluene is efficiently produced in Titan's atmosphere since C_6H_5, the main product of the photodissociation of benzene, reacts with the radicals most abundant in Titan's atmosphere, which are H and CH_3 [9]. However, molecular dinitrogen, in its closed shell electronic configuration, cannot react with hydrocarbons in the atmosphere of Titan because of the presence of relatively high activation energy barriers. In the upper atmosphere of Titan, however, molecular dinitrogen can be converted into atomic nitrogen or ions by energetic processes [10] or by the interaction with Extreme Ultra-Violet (EUV) radiation. The dissociation of molecular dinitrogen induced by dissociative photoionization, galactic cosmic ray absorption, N_2^+ dissociative recombination, or dissociation induced by EUV photons produces atomic nitrogen in its electronic ground state ^{4}S and in the first excited ^{2}D state in similar amounts [10]. While atomic nitrogen in its ^{4}S ground state exhibits very low reactivity with closed shell molecules, atomic nitrogen in its first electronically excited ^{2}D state shows a significant reactivity with several molecules identified in the atmosphere of Titan. Atomic nitrogen in its excited ^{2}D state is metastable but it shows a radiative lifetime long enough to react in binary collisions with other constituents of the upper atmosphere of Titan (6.1×10^4 s and 1.4×10^5 s for the $^2D_{3/2}$ and $^2D_{5/2}$ state, respectively) [11–19]. We have already investigated the reactions of atomic nitrogen in its excited ^{2}D state with aliphatic hydrocarbons, like CH_4, C_2H_2, C_2H_4, C_2H_6, in laboratory experiments by the crossed molecular beam technique and by ab initio and kinetics calculations [20–25]. More recently, with the same approach, we started the investigation of the reaction between N(^{2}D) and aromatic hydrocarbons like benzene [26]. In this study we will report preliminary calculations on the interaction of N(^{2}D) with benzene and toluene paying attention to the computational requirements. Indeed, the ab initio study of these systems is computationally very challenging and a compromise between chemical accuracy and computational resources is necessary.

2 Computational Details

The reactive channels of the N(^{2}D) + C_6H_6 and $C_6H_5CH_3$ systems leading to the insertion of atomic nitrogen into a C—H or C—C bond were investigated by locating the lowest stationary points at the B3LYP level of theory [27, 28], in conjunction with the 6 − 311 + G** basis set [29, 30], on the doublet ground state potential energy surface. The basis set superposition error (BSSE) has been estimated using the counterpoise method [31, 32]. At the same level of theory we have computed the harmonic vibrational frequencies in order to check the nature of the stationary points, *i.e.* minimum if all the frequencies are real, saddle point if there is only one imaginary

frequency. The assignment of the saddle points was performed using intrinsic reaction coordinate (IRC) calculations [33, 34] The geometry of all the species was optimized without any symmetry constraints considering for all the investigated species the electronic ground state. In order to check the accuracy of the computed geometries, we have optimized all the minima using a more extended basis set. We have optimized all the minima at the B3LYP level [27, 28] with the correlation consistent aug-cc-pVTZ basis set [35]. For all the stationary points, the energy was computed also at the higher level of calculation CCSD(T) [36–38] using the same correlation consistent aug-cc-pVTZ basis set [35] and the B3LYP/aug-cc-pVTZ optimized geometries, following a well established computational scheme [39–49]. The accuracy of the employed approach, in particular as far as basis set completeness is concerned, has been recently investigated [50]. Both the B3LYP and the CCSD(T) energies were corrected to 0 K by adding the zero point energy correction computed using the scaled harmonic vibrational frequencies evaluated at B3LYP level. The energy of N(^{2}D) was estimated by adding the experimental [51] separation N(^{4}S) – N(^{2}D) of 55 kcal mol^{-1} to the energy of N(^{4}S) at all levels of calculation. All calculations were done using Gaussian 09 [52] while the analysis of the vibrational frequencies was performed using Molekel [53, 54].

3 Results and Discussion

Figure 1 reports the optimized geometries of the stationary points localized along the reactive channel leading from N(^{2}D) + benzene to the insertion product of N(^{2}D) into a C—H bond and finally to the formation of the imidogen radical NH. We have found four minima along this reaction channel connected by three transition states: the first minimum (**1**) is only an adduct where N is slightly interacting with the benzene ring; the second one (**2**) shows a C atom of the ring bonded to an H and the N atoms; the third minimum (**3**) shows the nitrogen atom bonded to two adjacent carbon atoms and then the fourth minimum (**4**) shows the insertion of the nitrogen atom into the C—H bond with the formation of an NH group. Figure 1 shows the main geometrical parameters optimized at B3LYP level using both the 6 − 311 + G** and the aug-cc-pVTZ basis set. The last results are reported in parentheses. Some of these optimized structures were previously reported [55]. We can notice that there is a good agreement between the geometries optimized with the 6 − 311 + G** and the aug-cc-pVTZ basis set, the differences being within 0.01Å. There is only one relevant difference represented by the N—C distance in species **1**: this distance indeed is 3.044 Å with the 6 − 311 + G** basis set and 3.186 Å with the aug-cc-pVTZ basis set. However, this is an adduct and the energy dependence from the distance in this case is weak, so it is very difficult to compute the correct bond length. In Fig. 2 we have reported the minimum energy path for the channel leading to species **4** and then to the formation of the imidogen radical. The approach of the nitrogen to the benzene ring leads to the adduct **1** which is more stable than the reactants by 30.1 kcal/mol. This species,

through the transition state **TS12** which is still well under the reactants gives rise to species **2** where we have a true C—N bond. Species **2**, through a very small barrier of only 0.1 kcal/mol evolves towards species **3** which shows the nitrogen bridging two adjacent carbon atoms. It is necessary to overcome a barrier of 48.4 kcal/mol for species **3** to evolve to the more stable species **4** which represents the lowest minimum in this path. Species **4** shows the insertion of the nitrogen into a C—H bond. The dissociation of the C—N bond leads to the formation of the imidogen radical in a process endothermic by 101.2 kcal/mol. The imidogen radical can be formed also by direct abstraction of the hydrogen by the N(^{2}D). If the nitrogen approaches the benzene ring from the hydrogen side, the adduct **5** is formed which is 30.0 kcal/mol more stable than the reactants. This adduct, through a transition state which is 22.7 kcal/mol under the reactants gives the products.

The direct abstraction of hydrogen implies only one step for the formation of the imidogen radical, while the reaction path through species **4** implies several steps which lie however at lower energies. In order to state which one is the preferred path, kinetic calculations are necessary and they will be performed in the future.

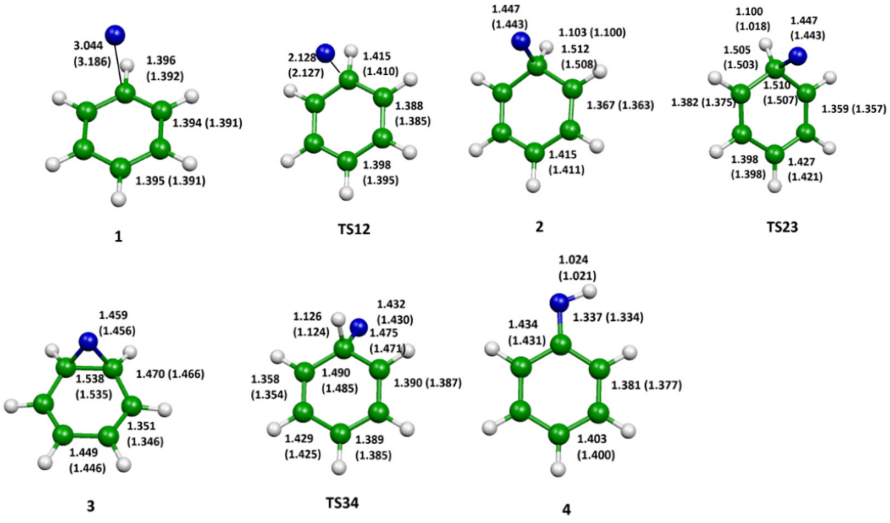

Fig. 1. Optimized geometries at B3LYP/6 − 311 + G** and B3LYP/aug-cc-pVTZ (in parentheses) level of the stationary points considered along the minimum energy paths leading from N(^{2}D) + C_6H_6 to C_6H_5NH. Bond lengths in Å.

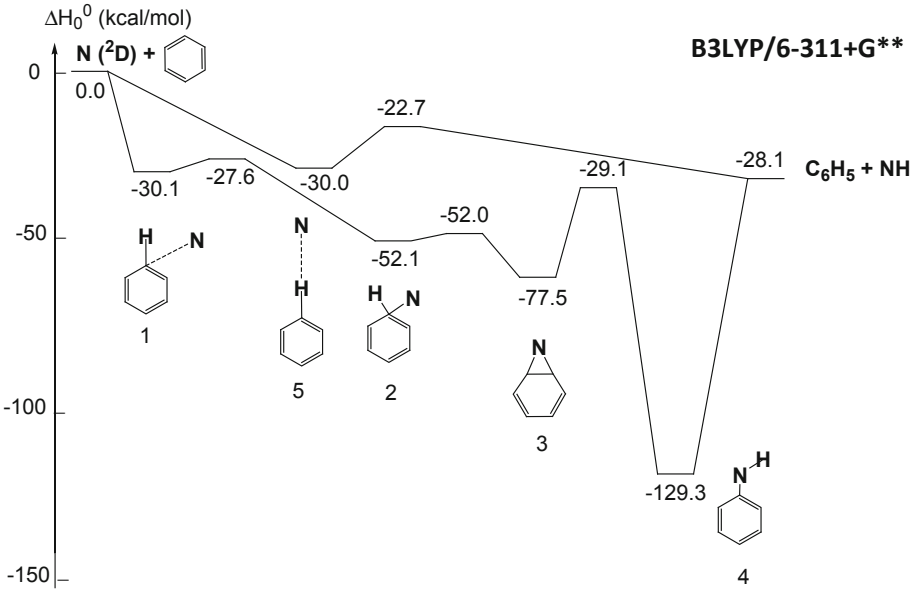

Fig. 2. Main steps along the minimum energy path for the channel leading to C_6H_5NH. Relative energies (kcal/mol, 0 K) with respect to the reactants $N(^2D) + C_6H_6$ computed at B3LYP/6 − 311 + G** level.

Figure 3 reports the optimized geometries of the stationary points localized along the reactive channel leading from $N(^2D)$ + toluene to the insertion product of $N(^2D)$ into a C—C bond and finally to the formation of the NCH_3 radical. We have found three minima along this reaction channel connected by two transition states: the first minimum **1** is only an adduct where N is slightly interacting with the toluene ring, being the C—N distance as high as 3.027 Å; the second one **2** shows the nitrogen atom bonded to two adjacent carbon atoms and then the third minimum **3** shows the insertion of the nitrogen atom into the C—C bond with the formation of an NCH_3 group. Figure 3 shows the main geometrical parameters optimized at B3LYP level using both the 6 − 311 + G** and the aug-cc-pVTZ basis set. The last results are reported in parentheses. We were not able to optimize the initial adduct at the B3LYP/aug-cc-pVTZ level. From Fig. 3 we can notice that there is a good agreement between the geometries optimized with the 6 − 311 + G** and the aug-cc-pVTZ basis set, the differences being within 0.01Å. We can also notice that the presence of the methyl substituent in toluene, with respect to benzene, changes the electronic distribution around the carbon atom, preventing the formation of the equivalent of species **2** reported in Fig. 1. In Fig. 4 we have reported the minimum energy path for the channel leading to species **3** and then to the formation of the NCH_3 radical. The approach of the

nitrogen to the ipso carbon of the toluene ring leads to the adduct **1** which is more stable than the reactants by 30.2 kcal/mol. This species, through the transition state **TS12** which is still well under the reactants gives rise to species **2** which shows the nitrogen bridging the ipso and the ortho carbon atoms. It is necessary to overcome a barrier of 47.5 kcal/mol for species **2** to evolve to the more stable species **3** which represents the lowest minimum in this path. Species **3** shows the insertion of the nitrogen into a C—C bond. The dissociation of the C—N bond leads to the formation of the NCH_3 radical in a process endothermic by 88.5 kcal/mol. Comparing Fig. 2 and Fig. 4 we can notice that, except for the presence of minimum **2** in Fig. 2 which, however, can evolve to minimum **3** through an almost negligible barrier height, the insertions of N(^{2}D) into a C—H or a C—C bond are very similar processes. Moreover, this seems to be a realistic path to the formation of a imidogen or a NCH_3 radical.

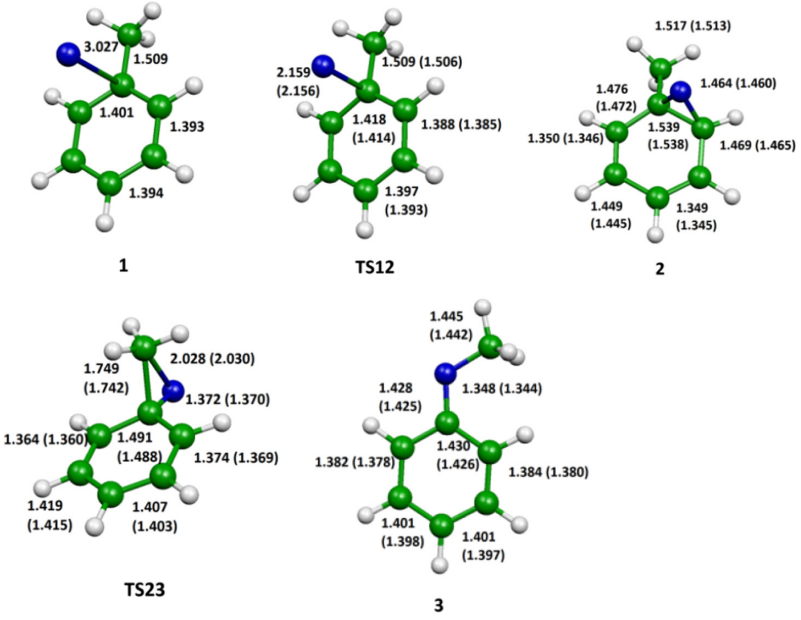

Fig. 3. Optimized geometries at B3LYP/6 − 311 + G** and B3LYP/aug-cc-pVTZ (in parentheses) level of the stationary points considered along the minimum energy path leading from N(^{2}D) + toluene to $C_6H_5NCH_3$. Bond lengths in Å.

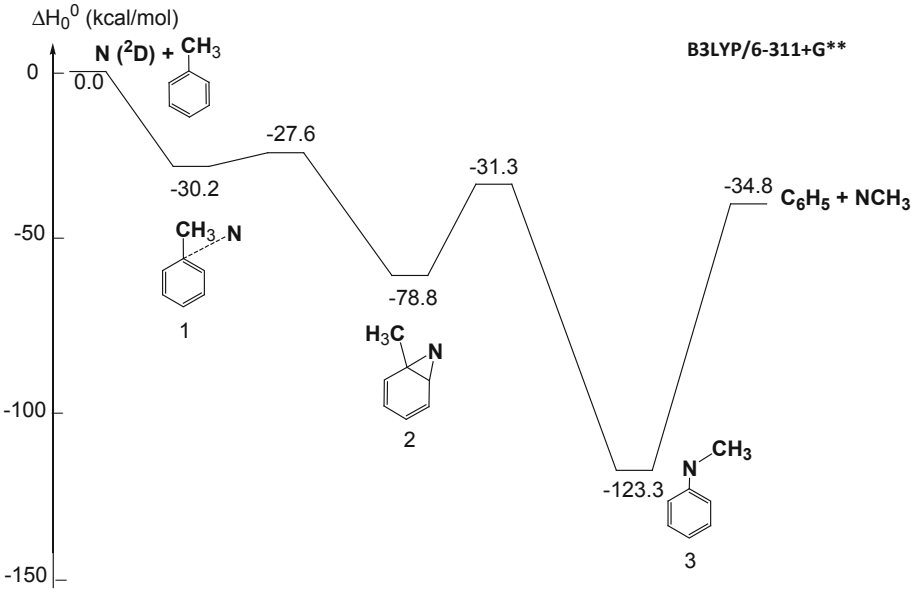

Fig. 4. Main steps along the minimum energy path for the channel leading to $C_6H_5NCH_3$. Relative energies (kcal/mol, 0 K) with respect to the reactants $N(^2D) + C_6H_5CH_3$ computed at B3LYP/6 − 311 + G** level.

Although, both in Fig. 2 and Fig. 4 all the species, including the transition states, are in energy well under the reactants, some doubts could emerge due to the low level of accuracy of the performed calculations. For this reason, we performed more accurate calculations using the CCSD(T) method in conjunction with a more extended basis set as the aug-cc-pVTZ. We optimized all the stationary points (minima and saddle points) at the B3LYP/aug-cc-pVTZ level and at these optimized geometries we performed CCSD(T)/aug-cc-pVTZ calculations. The energies of main steps along the minimum energy path for the reaction $N(^2D)$ + benzene → C_6H_5 + NH and $N(^2D)$ + toluene → C_6H_5 + NCH_3 are reported in Table 1. For the main processes we reported both the enthalpy differences and the barrier heights computed at 0 K. In Table 1, the first entry is the energy computed at B3LYP/6 − 311 + G**, the second entry the relative energy computed at B3LYP/aug-cc-pVTZ level and the third entry the energy computed at CCSD(T)/aug-cc-pVTZ//B3LYP/aug-cc-pVTZ level. We were not able to optimize the geometry of species **1** for the toluene reaction at the B3LYP/aug-cc-pVTZ level. For this reason, in Table 1 we have reported also the reaction from the reactants to species **2**.

Table 1. Enthalpy changes and barrier heights (kcal/mol, 0 K) computed at the B3LYP/6 − 311 + G**, B3LYP/aug-cc-pVTZ and CCSD(T)/aug-cc-pVTZ//B3LYP/aug-cc-pVTZ level of theory for the minimum energy path for the reactions N(^{2}D) + C_6H_6 → C_6H_5 + NH and N(^{2}D) + $C_6H_5CH_3$ → C_6H_5 + NCH_3. First entry B3LYP/6 − 311 + G**, second entry B3LYP/aug-cc-pVTZ and third entry CCSD(T)/aug-cc-pVTZ//B3LYP/aug-cc-pVTZ

	ΔH_0^0	Barrier height
Benzene		
N(^{2}D) + C_6H_6 → 1	−30.1, −31.2, −39.7	
1 → 2	−22.0, −21.4, −4.1	2.5, 2.7, 18.2
N(^{2}D) + C_6H_6 → 2	−52.1, −52.6, −43.8	−27.6, −28.5, −21.5
2 → 3	−25.4, −26.1, −30.2	0.1, 0, 0.3
3 → 4	−51,8, −52.2, −46.5	48.4, 48.7, 48.1
4 → C_6H_5 +NH	101.2, 101.8, 101.7	
Toluene		
N(^{2}D) + $C_6H_5CH_3$ → 1	−30.2	
1 → 2	−48.6	2.6
N(^{2}D) + $C_6H_5CH_3$ → 2	−78.8, −79.8, −75.9	−27.6, −28.3, −22.3
2→ 3	−44.5, −45.2, −37.4	47.5, 47.4, 54.0
3 → C_6H_5 + NCH_3	88.5, 89.1, 93.7	

Comparing the values of Table 1 we can notice that the B3LYP/6 − 311 + G** and the B3LYP/aug-cc-pVTZ energies differ always by a small amount of energy (around 1 kcal/mol). This difference is essentially due to the basis set superposition error computed with the counterpoise method which is 1.1 kcal/mol [31, 32]. Therefore, comparing the geometries and the energies, we can conclude that it is worthless to use a more extended basis set, with respect to the 6 − 311 + G**, to optimize the geometries at B3LYP level. Comparing the B3LYP and CCSD(T) energies we have a complete different situation, being the difference sometimes higher than ten kcal/mol. In particular, the difference between B3LYP and CCSD(T) energies is relevant for reactions involving species **1**: this is an expected result since species **1** is an adduct which is very difficult to describe accurately at B3LYP level; moreover, in species **1** there is a N(^{2}D) atom almost unperturbed and it is well known that the B3LYP method cannot describe correctly the nitrogen excited ^{2}D state.

For the reactions considered in this context, the situation however does not change dramatically going from B3LYP to CCSD(T) results because the energies of all the species investigated are still well under the reactants, but for other reaction this point could be very relevant.

4 Conclusions

The study at ab initio level of the reactions N(^{2}D) + C_6H_6 → C_6H_5 + NH and N(^{2}D) + $C_6H_5CH_3$ → C_6H_5 + NCH_3, performed using different methods in order to find a reasonable compromise between chemical accuracy and computational costs

suggests that, while for geometry optimizations even relatively low level calculations are adequate, for energies, calculations of higher level are necessary in order to obtain accurate quantitative results.

Acknowledgments. This work has been supported by MIUR "PRIN 2015" funds, project "STARS in the CAOS (Simulation Tools for Astrochemical Reactivity and Spectroscopy in the Cyberinfrastructure for Astrochemical Organic Species)", Grant Number 2015F59J3R. We acknowledge the Italian Space Agency for co-funding the Life in Space Project (ASI N. 2019-3-U.O). SF and MR acknowledge the project "Indagini teoriche e sperimentali sulla reattività di sistemi di interesse astrochimico" funded with Fondo Ricerca di Base 2018 of the University of Perugia. M.R. thanks the Dipartimento di Ingegneria Civile e Ambientale of the University of Perugia for allocated computing time within the project "Dipartimenti di Eccellenza 2018-2022".

References

1. Hörst, S.M.: Titan's atmosphere and climate. J. Geophys. Res. Planets **122**, 432–482 (2017)
2. Vuitton, V., Yelle, R.V., Anicich, V.G.: The nitrogen chemistry of Titan's upper atmosphere revealed. Astrophys. J. **647**, L175–L178 (2006)
3. Vuitton, V., Dutuit, O., Smith, M.A., Balucani, N.: Chemistry of Titan's atmosphere. In: Mueller-Wodarg, I., Griffith, C., Lellouch, E., Cravens, T. (eds.) Titan: Surface, Atmosphere and Magnetosphere. Cambridge University Press, Cambridge (2013)
4. Balucani, N.: Elementary reactions of N atoms with hydrocarbons: first steps towards the formation of prebiotic N-containing molecules in planetary atmospheres. Chem. Soc. Rev. **41**, 5473–5483 (2012)
5. Brown, R., Lebreton, J.P., Waite, J. (eds.): Titan from Cassini-Huygens. Springer, Netherlands (2010). https://doi.org/10.1007/978-1-4020-9215-2
6. Lai, J.C.-Y., et al.: Mapping vinyl cyanide and other nitriles in Titan's atmosphere using ALMA. Astron. J. **154**(206), 1–10 (2017)
7. Vuitton, V., Yelle, R.V., Cui, J.: Formation and distribution of benzene on Titan. J. Geophys. Res. **113**, E05007 (2008)
8. Clark, R.N., et al.: Detection and mapping of hydrocarbon deposits on Titan. J. Geophys. Res. **115**, E10005 (2010)
9. Loison, J.C., Dobrijevic, M., Hickson, K.M.: The photochemical production of aromatics in the atmosphere of Titan. Icarus **329**, 55–71 (2019)
10. Lavvas, P., et al.: Energy deposition and primary chemical products in Titan's upper atmosphere. Icarus **213**, 233–251 (2011)
11. Dutuit, O., et al.: Critical review of N, N^+, N_2^+, N^{++} and N_2^{++} main production processes and reactions of relevance to Titan's atmosphere. Astrophys. J. Suppl. Ser. **204**, 20 (2013)
12. Balucani, N.: Nitrogen fixation by photochemistry in the atmosphere of Titan and implications for prebiotic chemistry. In: Trigo-Rodriguez, J.M., Raulin, F., Muller, C., Nixon, C. (eds.) The Early Evolution of the Atmospheres of Terrestrial Planets, edited by Springer Series in Astrophysics and Space Science Proceedings, vol. 35, pp. 155–164 (2013). https://doi.org/10.1007/978-1-4614-5191-4_12
13. Balucani, N.: Elementary reactions and their role in gas-phase prebiotic chemistry. Int. J. Mol. Sci. **10**, 2304–2335 (2009)
14. Imanaka, H., Smith, M.A.: Formation of nitrogenated organic aerosols in the Titan upper atmosphere. PNAS **107**, 12423–12428 (2010)

15. Balucani, N., et al.: Dynamics of the N(^{2}D) + D_2 reaction from crossed-beam and quasiclassical trajectory studies. J. Phys. Chem. A **105**, 2414–2422 (2001)
16. Balucani, N., et al.: Experimental and theoretical differential cross sections for the N(^{2}D) + H_2 reaction. J. Phys. Chem. A **110**, 817–829 (2006)
17. Homayoon, Z., Bowman, J.M., Balucani, N., Casavecchia, P.: Quasiclassical trajectory calculations of the N(^{2}D) + H_2O reaction elucidating the formation mechanism of HNO and HON seen in molecular beam experiments. J. Phys. Chem. Lett. **5**, 3508–3513 (2014)
18. Balucani, N., Cartechini, L., Casavecchia, P., Homayoon, Z., Bowman, J.M.: A combined crossed molecular beam and quasiclassical trajectory study of the Titan-relevant N(^{2}D) + D_2O reaction. Mol. Phys. **113**, 2296–2301 (2015)
19. Israel, G., et al.: Complex organic matter in Titan's atmospheric aerosols from in situ pyrolysis and analysis. Nature **438**, 796 (2005)
20. Balucani, N., et al.: Combined crossed molecular beam and theoretical studies of the N(^{2}D) + CH_4 reaction and implications for atmospheric models of Titan. J. Phys. Chem. A **113**, 11138–11152 (2009)
21. Balucani, N., et al.: Cyanomethylene formation from the reaction of excited Nitrogen Atoms with Acetylene: A crossed beam and ab initio study. J. Am. Chem. Soc. **122**, 4443–4450 (2000)
22. Balucani, N., Cartechini, L., Alagia, M., Casavecchia, P., Volpi, G.G.: Observation of nitrogen-bearing organic molecules from reactions of nitrogen atoms with hydrocarbons: a crossed beam study of N(^{2}D) + ethylene. J. Phys. Chem. A **104**, 5655–5659 (2000)
23. Balucani, N.: Formation of nitriles and imines in the atmosphere of Titan: combined crossed-beam and theoretical studies on the reaction dynamics of excited nitrogen atoms N(^{2}D) with ethane. Faraday Discuss. **147**, 189–216 (2010)
24. Balucani, N., et al.: Combined crossed beam and theoretical studies of the N(^{2}D) + C_2H_4 reaction and implications for atmospheric models of Titan. J. Phys. Chem. A **116**, 10467–10479 (2012)
25. Rosi, M., Falcinelli, S., Balucani, N., Casavecchia, P., Skouteris, D.: A theoretical study of formation routes and dimerization of methanimine and implications for the aerosols formation in the upper atmosphere of Titan. In: Murgante, B., et al. (eds.) ICCSA 2013. LNCS, vol. 7971, pp. 47–56. Springer, Heidelberg (2013). https://doi.org/10.1007/978-3-642-39637-3_4
26. Balucani, N., Pacifici, L., Skouteris, D., Caracciolo, A., Casavecchia, P., Rosi, M.: A theoretical investigation of the reaction N(^{2}D) + C_6H_6 and implications for the upper atmosphere of Titan. In: Gervasi, O., et al. (eds.) ICCSA 2018. LNCS, vol. 10961, pp. 763–772. Springer, Cham (2018). https://doi.org/10.1007/978-3-319-95165-2_53
27. Becke, A.D.: Density functional thermochemistry. III. The role of exact exchange. J. Chem. Phys. **98**, 5648–5652 (1993)
28. Stephens, P.J., Devlin, F.J., Chablowski, C.F., Frisch, M.J.: Ab initio calculation of vibrational absorption and circular dichroism spectra using density functional force fields. J. Phys. Chem. **98**, 11623–11627 (1994)
29. Krishnan, R., Binkley, J.S., Seeger, R., Pople, J.A.: Self-consistent molecular orbital methods. XX. A basis set for correlated wave functions. J. Chem. Phys. **72**, 650–654 (1980)
30. Frisch, M.J., Pople, J.A., Binkley, J.S.: Self-consistent molecular orbital methods 25 Supplementary functions for Gaussian basis sets. J. Chem. Phys. **80**, 3265–3269 (1984)
31. Simon, S., Duran, M., Dannesberg, J.J.: How does basis set superposition error change the potential surfaces for hydrogen-bonded dimers? J. Chem. Phys. **105**, 11024–11031 (1996)
32. Boys, S.F., Bernardi, F.: The calculation of small molecular interactions by the differences of separate total energies Some procedures with reduced errors. Mol. Phys. **19**, 553–566 (1970)

33. Gonzalez, C., Schlegel, H.B.: An improved algorithm for reaction path following. J. Chem. Phys. **90**, 2154–2161 (1989)
34. Gonzalez, C., Schlegel, H.B.: Reaction path following in mass-weighted internal coordinates. J. Phys. Chem. **94**, 5523–5527 (1990)
35. Dunning Jr., T.H.: Gaussian basis sets for use in correlated molecular calculations. I. The atoms boron through neon and hydrogen. J. Chem. Phys. **90**, 1007–1023 (1989)
36. Bartlett, R.J.: Many-body perturbation theory and coupled cluster theory for electron correlation in molecules. Annu. Rev. Phys. Chem. **32**, 359–401 (1981)
37. Raghavachari, K., Trucks, G.W., Pople, J.A., Head-Gordon, M.: Quadratic configuration interaction. A general technique for determining electron correlation energies. Chem. Phys. Lett. **157**, 479–483 (1989)
38. Olsen, J., Jorgensen, P., Koch, H., Balkova, A., Bartlett, R.J.: Full configuration–interaction and state of the art correlation calculations on water in a valence double-zeta basis with polarization functions. J. Chem. Phys. **104**, 8007–8015 (1996)
39. de Petris, G., Cacace, F., Cipollini, R., Cartoni, A., Rosi, M., Troiani, A.: Experimental detection of theoretically predicted N_2CO. Angew. Chem. **117**, 466–469 (2005)
40. De Petris, G., Rosi, M., Troiani, A.: SSOH and HSSO radicals: an experimental and theoretical study of $[S_2OH]^{0/+/-}$ species. J. Phys. Chem. A **111**, 6526–6533 (2007)
41. Bartolomei, M., et al.: The intermolecular potential in $NO\text{-}N_2$ and $(NO\text{-}N_2)^+$ systems: implications for the neutralization of ionic molecular aggregates. PCCP **10**, 5993–6001 (2008)
42. Leonori, F., et al.: Observation of organosulfur products (thiovinoxy, thioketene and thioformyl) in crossed-beam experiments and low temperature rate coefficients for the reaction $S(^1D) + C_2H_4$. PCCP **11**, 4701–4706 (2009)
43. Leonori, F., et al.: Crossed-beam and theoretical studies of the $S(^1D) + C_2H_2$ reaction. J. Phys. Chem. A **113**, 4330–4339 (2009)
44. De Petris, G., Cartoni, A., Rosi, M., Barone, V., Puzzarini, C., Troiani, A.: The proton affinity and gas-phase basicity of sulfur dioxide. ChemPhysChem **12**, 112–115 (2011)
45. Berteloite, C., et al.: Low temperature kinetics, crossed beam dynamics and theoretical studies of the reaction $S(^1D) + CH_4$ and low temperature kinetics of $S(^1D) + C_2H_2$. Phys. Chem. Chem. Phys. **13**, 8485 (2011)
46. Rosi, M., Falcinelli, S., Balucani, N., Casavecchia, P., Leonori, F., Skouteris, D.: Theoretical study of reactions relevant for atmospheric models of Titan: rocarbons. In: Murgante, B., et al. (eds.) ICCSA 2012. LNCS, vol. 7333, pp. 331–344. Springer, Heidelberg (2012). https://doi.org/10.1007/978-3-642-31125-3_26
47. Skouteris, D., Balucani, N., Faginas-Lago, N., Falcinelli, S., Rosi, M.: Dimerization of methanimine and its charged species in the atmosphere of Titan and interstellar/cometary ice analogs. Astron. Astrophys. **584**, A76 (2015)
48. Falcinelli, S., Rosi, M., Cavalli, S., Pirani, F., Vecchiocattivi, F.: Stereoselectivity in autoionization reactions of hydrogenated molecules by metastable gas atoms: the role of electronic couplings. Chemistry Eur. J. **22**, 12518–12526 (2016)
49. Troiani, A., Rosi, M., Garzoli, S., Salvitti, C., de Petris, G.: Vanadium hydroxide cluster ions in the gas phase: bond-forming reactions of doubly-charged negative ions by SO_2-promoted V-O activation. Chem. Eur. J. **23**, 11752–11756 (2017)
50. Rosi, M., et al.: An experimental and theoretical investigation of 1-butanol pyrolysis. Front. Chem. **7**, 326 (2019). https://doi.org/10.3389/fchem.2019.00326
51. Moore, C.E.: Atomic Energy Levels, Natl. Bur. Stand. (U.S.) Circ. N. 467 (U.S., GPO, Washington, DC, 1949)
52. Gaussian 09, Revision A.02, Frisch, M.J., et al.: Gaussian, Inc., Wallingford CT (2009)

53. Flükiger, P., Lüthi, H. P., Portmann, S., Weber, J.: MOLEKEL 4.3, Swiss Center for Scientific Computing, Manno (Switzerland), 2000–2002
54. Portmann, S., Lüthi, H.P.: MOLEKEL: an interactive molecular graphics tool. Chimia **54**, 766–769 (2000)
55. Balucani, N., et al.: A computational study of the reaction N(^{2}D) + C_6H_6 leading to pyridine and phenylnitrene. In: Misra, S., et al. (eds.) ICCSA 2019. LNCS, vol. 11621, pp. 316–324. Springer, Cham (2019). https://doi.org/10.1007/978-3-030-24302-9_23